

# Influence of Impact Effect in Bidirectional UPSS Bearing

Xinhao He

*Department of Urban Management  
Graduate School of Engineering  
Kyoto University  
Kyoto, Japan  
he.xinhao.25u@st.kyoto-u.ac.jp*

Akira Igarashi

*Disaster Prevention Research Institute  
Kyoto University  
Kyoto, Japan  
igarashi.akira.7m@kyoto-u.ac.jp*

**Abstract**—The Uplifting Sliding Shoe (UPSS) bearing is a type of friction bearing proposed to ensure a sufficient seismic performance and to provide a cost saving solution for the thermal expansion and contraction of the multi-span continuous girder bridges. The use of multiple sliding surfaces of specific geometric shape is the main feature of UPSS to effectively provide restoring force in the event of strong earthquakes. Since impact force caused by the boundary region between two sliding surfaces is one of the critical factor in the design, the influence of the impact force on the seismic response of the bridge is investigated for the bidirectional application of UPSS in the bridge system in the present study. A two-phase analysis procedure is introduced to provide a reasonable discussion of the impact effect. In the first step, a rigorous modelling of UPSS based on the dynamic equilibrium analysis with a tubular arc in the boundary areas of the sliding surfaces is shown to control the intensity of impact. In the second step, a multiple spring model with various boundary properties is used to confirm the results of the first step and to investigate the impact effect in a quantitative manner. The study indicates that the bearing displacement response of the bidirectional UPSS is relatively robust so that the influence of the assumed boundary conditions is regarded as minor, while the simplified model is likely to overestimate the bearing displacement response compared with the multiple springs model. Furthermore, the potential impact effect can result in uncertainty to the pier response ductility factor.

**Keywords**—Uplifting slide shoe, seismic bearing, impact modelling, bidirectional condition

## I. INTRODUCTION

The seismic pounding damage in the bridge systems has been repetitively observed in many previous investigations. Evidences from the Kobe earthquake in 1995 [1] indicate the serviceability of bridge can be damaged by the pounding as a result of collisions among girders. Even though the energy dissipation devices, like the damper, can be used to mitigate seismic response, for the bridge systems with the use of seismic bearings, collision problems are still inevitable in large earthquakes due to the excessive structural deformation and bearing displacement. Most of studies regarding the pounding generated in bridge systems focus on the longitudinal response, it is recognized that significant lateral pounding can also result in excessive girder displacement or even unseating.

As an effective and economical seismic protection approach for multi-span continuous girder bridges, the Uplifting Slide Shoe (UPSS) is useful in dispersing the influence of thermal expansion and contraction of the bridge girders to multiple piers and seismic enhancement [2, 3]. In

the conventional design practice for the regular shape bridge systems with the application of UPSS devices, the side blocks or restrainers are assumed to be implemented in the transverse direction so as to restrain the transverse displacement and to avoid the falling accident of the girders. Because the nature of ground motion is of three-dimension with the major influence of the horizontal plane on the structural horizontal characteristics, in the irregular shape bridge systems, the seismic measures also need to be considered to be adopted to the transverse direction. When considering the transverse implementation of the elastomeric bearings or other supplementary devices to provide additional restoring force in conjunction with the longitudinal implementation of UPSS devices in a single span, the variation of vertical displacement caused by the uplifting motion of UPSS will cause problems for the application of elements without vertical mobility. Therefore, the implementation of UPSS is extended to the application in the bidirectional condition to provide a sufficient bidirectional seismic performance. The use of multiple sliding surfaces in form of specific geometric shape is the main feature of UPSS to effectively provide restoring force in the event of strong earthquakes. However, the significant impulsive force, or pounding process, is observed in the boundary area between its different sliding surfaces due to its peculiar geometry based on past unidirectional tests [4]. It is concerned that this phenomenon may result in uncertainties of bearing dynamic response. For the further application of UPSS in the bridge systems, it becomes necessary to investigate the influence of impact effect not only in the unidirectional condition but also in a bidirectional condition.

Extensive efforts have been made in order to examine or to avoid the adverse influence induced by the pounding process. The past studies for the pounding influence between adjacent buildings [5-7] indicate that pounding can result in displacement amplification, which is mainly related to the period and mass of the building next to it. Their studies also pointed out that the pounding influence is not sensitive to the change of the stiffness of the impact elements, simulating the collisions. According to the examination of adjacent pounding structures in both steady-state and transient excitations, Wolf et al. emphasized that the pounding hardly changes the global seismic response [5]. Robert et al. studied the pounding of superstructure segments in the isolated bridge showed that collisions have considerable influence, especially, in the longitudinal direction of the bridge [8]. But the pounding patterns are not significantly sensitive to the choice of impact element damping. Deepak et al. investigated the bidirectional response of base-isolated buildings considering pounding with

retaining walls [9]. It is concluded that the peak base displacements can be amplified under near-fault motions compared with far-fault motions. Furthermore, the floor acceleration and the difference between bidirectional and unidirectional excitations may increase due to pounding. Eftychia underlined the influence of spatial earthquake-induced pounding in the base-isolated buildings pounding against moat walls [10]. Yu et al. focused on the effect of the restraining rim on the extreme behavior of pendulum sliding bearings [11]. It is found that bearings without rims induce the lowest force but largest horizontal displacement and the impact force has a significant influence in the stiff superstructure than in the flexible superstructures.

The impact is regarded as a process which is most significant in the field of multi-body dynamics experiencing contact for an infinitesimal time duration in the modelling. Due to the inherent uncertainties caused in pounding such as unknown geometries of the contact area, uncertain properties of material under the impact and variable impact incident velocities, the study of pounding is required to consider parametric variation of the impact element. Several impact modelling methods have been proposed to simulate pounding [12, 13], which can be categorized as: the stereo-mechanic method (impulsive-based method); the contact element method (force-based method); and the arbitrary bodies/surfaces contact method. Using the impulsive-momentum law, Goldsmith developed the stereo-mechanic method to predict the velocities of one or two rigid bodies after pounding [14]. However, this method cannot provide the magnitude of pounding force and the duration of the collision as the results of its underlying assumption. The contact element method, which is a more popular method used in pounding modelling, is considered as a force-based approach. Several linear and nonlinear contact models have been developed with the use of the basic dashpot contact element and a gap, including the linear springs model [15, 16], the Hertz model with a nonlinear spring [17-21], the Hertz damp model accounting for the damping property [12, 19], and the Kelvin model [12, 20, 21]. With adjustment of the combination of the stiffness, the damping effect, and the gap size of the contact element, the contact element method is able to provide variable impact properties for the study of the influence of pounding under different circumstances. Because of the modelling procedure, the elements developed by the Kelvin model can easily be implemented into commercial structural software. It was reported that the impact models accounting for energy dissipation are suited for the pounding simulation [22, 23]. The arbitrary contact surface [24-30] is based on the point to surface contact with the consideration of material overlap. The detailed geometric information is required in this method to carry out the contact recognition. Although the task to search for the contact target is time consuming and the searching algorithm is complicated, it is reported by Bi et al. that when transverse ground motion and torsional response of the bridge decks are considered, a detailed 3-dimensional arbitrary contact model is more accurate than the results obtained from the stereo-mechanic method and the contact element method [12]. It is realized that the conservation of momentum and energy dissipation during the pounding are two critical indices to treat collision problem. More specifically, the conservation of momentum is related to the intensity of resisting force generated in this area in an infinitesimally short duration. The energy dissipation is a directly relevant index to represent the damping effect.

Although the contact element methods mentioned above are considered as a powerful and convenient approach to deal with the pounding problem, the main reason of choosing the impulsive-based approach is to avoid the uncertainties regarding the determination of the elements properties, including the impact spring stiffness and the damping ratio, which in fact is the major disadvantage of the force-based impact model method.

Although the unidirectional shake table test and the corresponding investigation have been carried out to discuss the impact issues of the UPSS bearing [4], it still lacks comprehensive study and understanding for the potential influence of the impact effect in a bidirectional condition. Due to the uncertainties of pounding and the lack of data validation, it is expected to offer a comprehensive study for this problem by determining the impact force and energy dissipation at different levels. Therefore, a two phase analysis is used to develop a reasonable discussion for this problem. In the first step, based on the dynamic equilibrium analysis, a simplified model is used to provide restoring force description for the Bidirectional UPSS. The impact force generated in the boundary areas of the sliding surfaces is provided as the centrifugal force by the superimposed tubular arc, which is shown to control the intensity and energy dissipation of the impact process by assigning a specific radius value and a width of superimposed area. It is assumed that the potential influence of the impact effect is studied in an incremental and qualitative manner due to its rigorous modelling concept. This model is essentially a force-based model, but it also possesses both the characteristics of impulsive-based method and arbitrary surfaces method, including a low uncertainty of the impact effect and the utility of the detailed geometric information. In the second step, a multiple spring model of UPSS with various boundary properties is used to confirm the results of first step and to study the influence of pounding in a quantitative manner due to its capability of describing the three-dimensional behavior of UPSS bearing in a practical manner. Incorporating the two phase analysis mentioned above, a comprehensively parametric study is carried out by using a global response index to quantify the sensitivity of the bearing behavior to the impact effect. Furthermore, as a seismic approach in the bridge system, the potential influence of the impact effect of UPSS on the piers response ductility is also investigated following the same idea with the aid of the dynamic equilibrium modelling procedure.

## II. MODELLING AND GROUND MOTION

The mechanism of UPSS consists of friction and restoring force induced by gravity loads between the sliding surfaces and a slider for seismic response control. The unique feature of the nonlinear hysteresis behavior of UPSS is determined by the multi-sliding surface configuration consisting of a horizontal plane and two inclined slopes as shown in Fig. 2.1. The character of the sliding surfaces can be specified by three primary parameters: the frictional coefficient between the contact surface and the slider material ( $\mu$ ), the angle of the inclined surfaces ( $\theta$ ), and the clearance ( $L$ ) implying the sliding distance from the neutral position on the horizontal plane to either of beginning of the slopes.

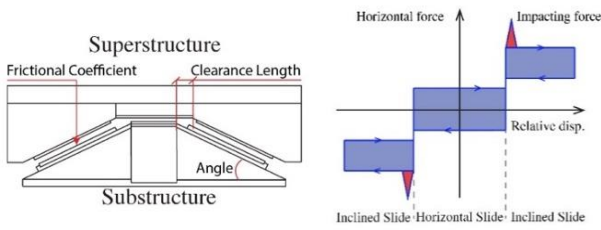


Fig. 2.1. Mechanical characteristics of UPSS

It is reasonable to postulate that flexibility and rotation of the girder are neglected implying so that the superstructure is reasonably modeled as a lumped mass with three translational degrees of freedom. A simplified multi-degree-of-freedom (MDOF) model for a single girder supported by the Bidirectional UPSS system is shown in Fig. 2.2. The Bidirectional UPSS is eventually represented by an integrated five-slide-plane friction device model. When the Bidirectional UPSS is set into motion, the bidirectional restoring force can be provided by any of the sliding surfaces, which depends on the geometric contact condition between the superstructure and the Bidirectional UPSS device.

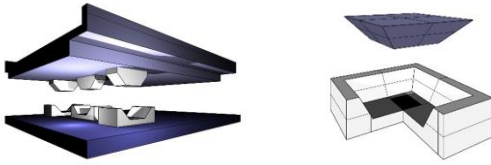


Fig. 2.2. Simplified Bidirectional UPSS model with a rigid superstructure

#### A. Dynamic Equilibrium Condition in Any Sliding Surface

A straightforward solution for the determination of the dynamic status system is determined by dynamic equilibrium analysis. In the present study, the origin point of coordinates is fixed on the ground. It is assumed that the motion trajectory of the superstructure can perfectly slide along the geometric shape of the bearing as a rigid body motion without separation. The magnitude of friction force is proportional to the resistant force on current sliding surface with the assumption of Coulomb model.

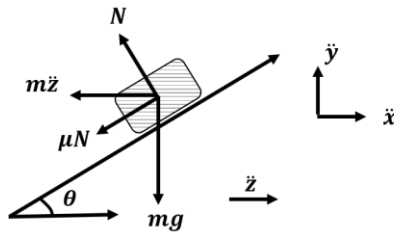


Fig. 2.3. Simplified rigid body model in dynamic equilibrium condition

For example, when the superstructure is sliding on the positive slope surface in the  $x$  direction and the acceleration of ground motion  $\ddot{z}$  takes place as shown in the Fig. 2.3, the dynamic equilibrium relationship with the compatibility requirement can be expressed as (1):

$$\begin{cases} x: -m\ddot{z} - \mu N \cos\theta - N \sin\theta = m\ddot{x} \\ y: N \cos\theta - mg - \mu N \sin\theta = m\ddot{y} \\ x,y: \tan\theta = \dot{y}/\dot{x} \end{cases} \quad (1)$$

where the  $N$  is the resistant force,  $\ddot{x}$ ,  $\ddot{y}$  and  $\ddot{z}$  are the acceleration components in three directions.

Rearranging the equation yields the expression of resistant force as (2):

$$N = mg \cos\theta - m\ddot{z} \sin\theta \quad (2)$$

where the direction of  $N$  points to the direction normal to the slope, as shown in the figure.

#### B. Multiple Sliding Surface Model for Bidirectional UPSS

It is necessary to provide the geometric information to define the condition for activating the corresponding sliding surface and to determine the generated restoring force. The dynamic status of Bidirectional UPSS can be specified by a two-dimensional coordinate system on the horizontal plane since the dynamic equilibrium condition inherently determines the vertical motion.

The geometric information is defined as follows. As expressed in (3), let the  $[T_w]_j$ ,  $[T_p]_j$  and  $[T_n]_j$  be the column vectors of the  $j$ -th sliding surface in the  $w$ ,  $p$  and  $n$  directions of this surface, respectively. As shown in the Fig. 2.4, through a series of coordinate transformation, in the local coordinate system, the  $p$  direction is defined as the direction parallel to the working surface and pointing toward the central horizontal plane, which means that it is the transformation result of the  $x$  axis direction. The direction orthogonal to the  $p$  direction on the working surface is defined as the  $w$  direction, which means that it is the transformation result of the  $y$  axis direction. The direction orthogonal to the  $w$  and  $p$  direction on the working surface is defined as  $n$  direction, which means that it is the transformation result of the  $z$  axis direction. An example of the layout of the sliding surfaces and the coordinate system is shown in Fig. 2.4, in which the inclined surface located on the positive  $x$  direction is active, the corresponding  $p$  direction is pointed along the  $x$  coordinate and the  $w$  direction is defined in the direction of the positive  $y$  coordinate. The norm of these vectors is normalized to unity. The matrix  $[T]_j$  is defined as the combination of the three vectors.

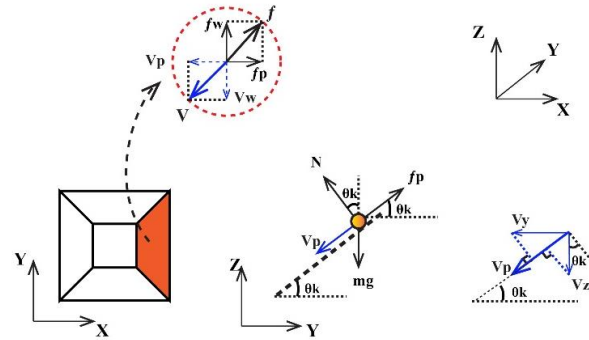


Fig. 2.4. Direction of force acting to a point mass sliding on an inclined sliding surface including coupled effect

$$\begin{aligned} [T_p]_j &= [T_{px} \quad T_{py} \quad T_{pz}]^T \\ [T_w]_j &= [T_{wx} \quad T_{wy} \quad T_{wz}]^T \\ [T_n]_j &= [T_{nx} \quad T_{ny} \quad T_{nz}]^T \\ [T]_j &= \begin{bmatrix} T_{px} & T_{py} & T_{pz} \\ T_{wx} & T_{wy} & T_{wz} \\ T_{nx} & T_{ny} & T_{nz} \end{bmatrix} \end{aligned} \quad (3)$$

The modelling procedure follows the flowchart shown in Fig 2.5:

- Identify the sliding surface to be triggered based on the specified geometry.
- The unit vector of the horizontal projection of the current sliding surface is extracted as  $\mathbf{S}$  by (4), which is used to determine the effective external load. The inner product of the projection vectors of the sliding surface in the  $p$  and  $n$  directions is computed as  $S2$  as in (5), which is used to determine the sign of the resistant force.

$$\mathbf{S} = [T_{px} \ T_{py} \ 0] / |[T_{px} \ T_{py} \ 0]| \quad (4)$$

$$S2 = [T_{px} \ T_{py} \ 0] \cdot [T_{nx} \ T_{ny} \ 0] \quad (5)$$

- Since the generated resistant force will be normal to the surface, the effective external load along the extracted direction  $\mathbf{S}$  for the ground acceleration is calculated as  $\ddot{z}$  in (6).

$$\ddot{z} = [a_x \ a_y \ 0] \cdot \mathbf{S} \quad (6)$$

where  $a_x$  and  $a_y$  are the  $x$ - $y$  components of the ground acceleration.

- The resistant force can be expressed as follows:

$$N = (mg + m\ddot{z}_v + F_v) \sqrt{T_{px}^2 + T_{py}^2} + \text{sign}(S2)(m\ddot{z}_{\text{ground}} + m\ddot{z}_{\text{sub}} + F_h) \text{abs}(T_{pz}) \quad (7)$$

where  $F_v$  and  $F_h$  are the effective vertical and horizontal components of the external force provided by other restoring elements of the bidirectional UPSS. The symbols  $\ddot{z}_{\text{ground}}$  and  $\ddot{z}_{\text{sub}}$  denote the effective accelerations corresponding to the ground motion and the substructure motion, respectively.

- The components of friction force obeying the circular coupled effect is determined with the Coulomb model.
- Finally, the horizontal restoring force in the global coordinates is determined by integrating the friction force and resistant force.

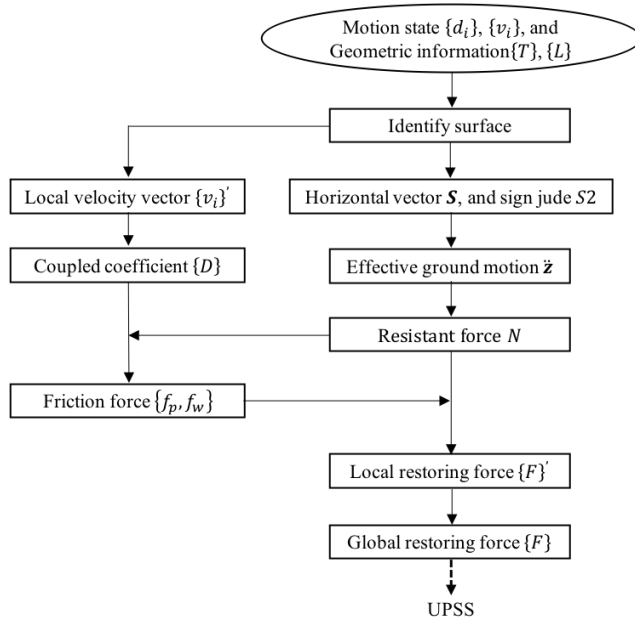


Fig. 2.5. Flowchart of restoring force determination for bidirectional UPSS

### C. Modelling of Impact Effect

Due to the lack of experimental data, the potential influence of impact effect is considered in the modelling. The impact process with controllable intensity and energy dissipation is assumed in the developed model. The regions related to the impact effect are in the cross-section of the inclined planes and the boundary areas of inclined sliding surfaces, as shown in the Fig. 2.6.

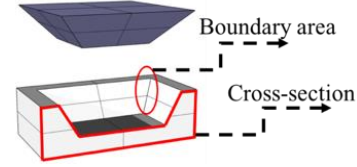


Fig. 2.6. The schematic of impact generated regions

A bird-eye view of the Bidirectional UPSS is shown in Fig. 2.7. The areas where the impact effect can occur are also the intersection line between adjacent surfaces indicated by black lines. By introducing a tubular arc as a superimposed element into the impact areas, the impact phenomenon with different intensities of centrifugal force can be described by adjusting its curvature radius. The energy dissipation is controlled by the width of boundary area where the impact element is activated in a strip-shaped zone near the intersection line between the two sliding surfaces,  $\pm s/2$ . The modelling procedure consists of the following steps and illustrated by the flowchart in Fig. 2.8:

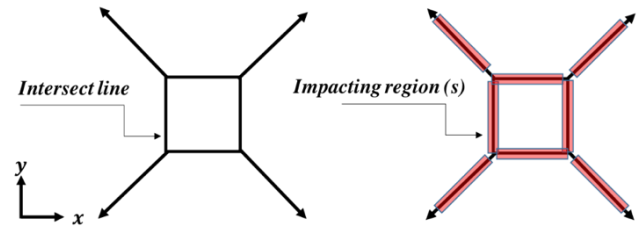


Fig. 2.7. The schematic of regions added with tubular arcs

- The activated impact region is identified among the eight possible regions shown in Fig. 2.7.
- The instantaneous direction of centrifugal force acting on the fictitious particle on the tubular arc is determined. The direction can be determined by the distance from the current location of the particle ( $d_x$ ,  $d_y$ ,  $d_z$ ) to the boundary line of the impact region in the horizontal plane. For example, when the superstructure is sliding across the boundary between the horizontal to the inclined surface in the positive  $x$  direction, this angle of the instantaneous direction of the centrifugal force  $\vartheta$  can be calculated by (8):

$$\vartheta = \frac{|d_x| - (L_x - \frac{s}{2})}{s} \varphi \quad (8)$$

where  $\varphi$  is the angle between the normal directions of the two sliding surfaces. In this case,  $\varphi$  coincides with the inclined angle of the slope  $\theta$ .

- The value of centrifugal force  $N$  is determined by (9).

$$N = m|v|^2/r \quad (9)$$

where the  $v$  is the velocity component orthogonal to the direction intersect line in the current surface and the  $r$  is radius of tubular arc.

- Finally, the relevant friction force component is determined and then the horizontal restoring force vector in the global coordinates is computed.

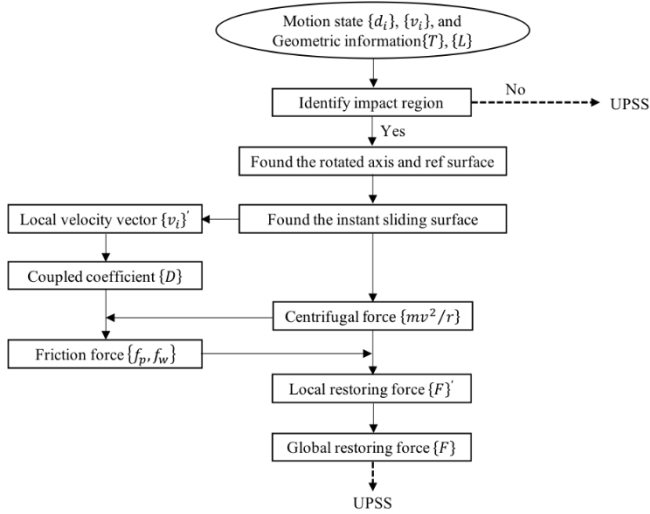


Fig. 2.8. Flowchart of impact force determination for Bidirectional UPSS

#### D. Input information

A suite of 18 pairs of horizontal bidirectional earthquake excitations obtained from the PEER and JMA strong motion database is used as input for the analyses in Table 2.1. The ground motion set employed was intended to cover a wide range of intensities and frequency content. The acceleration response spectra of the bidirectional ground motion record are shown in Fig. 2.9, in which the spectral acceleration is defined as the geometric square root of the two horizontal components.

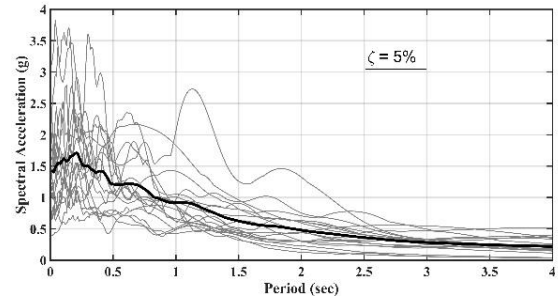


Fig. 2.9. The spectral acceleration of 18 ground motion records with 5% damping ratio

TABLE 2.1: THE LIST OF GROUND MOTION RECORDS

No.	Earthquake Record	Component PGA(g)		M
		X direction	Y direction	
1	Cape Mendocino 4/25/1992	1.497	1.039	7.1
2	Chi-Chi Taiwan 9/20/1990	0.462	0.566	7.6
3	Coalinga 5/2/1983	0.592	0.551	6.4
4	Duzce, Turkey 11/12/1999	0.348	0.535	7.1
5	Erzincan, Turkey 3/13/1992	0.496	0.515	6.9
6	Galli, USSR 5/17/1976	0.608	0.717	6.8
7	Imperial Valley 10/15/1979	0.41	0.439	6.5
8	Irpinia, Italy 11/23/1980	0.251	0.358	6.5
9	Kobe 1/16/1995	0.611	0.615	6.9
10	Kocaeli, Turkey 8/17/1999	0.267	0.349	7.4
11	Landers 6/28/1980	0.785	0.721	7.3
12	Loma Prieta 10/18/1989	0.563	0.605	6.9
13	Morgan Hill 4/24/1984	0.711	1.298	6.2
14	N. Palm Springs 7/8/1986	0.594	0.694	6.0
15	Northridge 1/17/1994	0.837	0.472	6.7
16	San Fernando 2/9/1971	1.226	1.159	6.6
17	Superstition Hills 11/24/1987	0.455	0.377	6.7
18	Tabas, Iran 9/16/1978	0.836	0.852	7.4

### III. QUALITATIVE ANALYSIS OF IMPACT EFFECT

In the present study, the friction coefficient of the sliding surfaces and the clearance are assumed as  $\mu = 0.15$  and  $L = 30\text{mm}$ , respectively. The bearing response for the case of the inclined angle of  $20^\circ$  and the excitation of JMA Kobe record is shown in Fig. 3.1. A significant force spike generated in the boundary area can be observed when a radius of the tubular arc of  $50\text{mm}$  plotted with a blue line. The red line represents the case neglecting the impact force by assigning the radius as infinite.

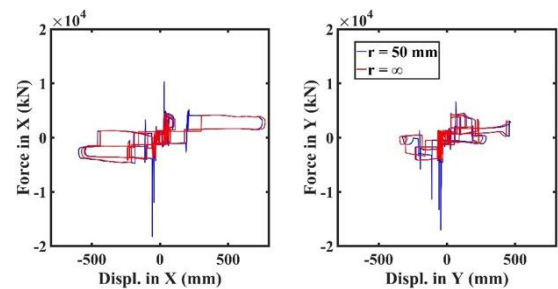
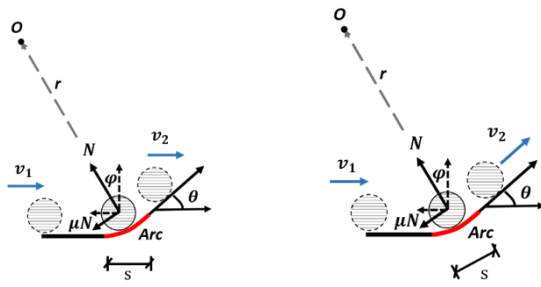


Fig. 3.1. The Bidirectional UPSS response under JMA Kobe excitation

The potential influence of the impact effect is investigated by controlling the radius of the tubular arcs or the width of superimposed area in an incremental manner. The impact effect can be separated into two aspects, the impact force and the energy loss. The energy loss in the boundary area of this simplified model is revealed by an iterative procedure.



(a). From horizontal to inclined plane  
(b). Between inclined sliding surfaces  
Fig. 3.2. The incident and exit situation of simplified model

Since this model provides only the horizontal description for the bearings behavior, the analysis of energy loss focuses on the energy exchange in the horizontal direction without considering the vertical component. Based on Fig. 3.2 (a), the horizontal components of resistant force  $N_h$  and friction force  $f_h$  when the superstructure moves across through the boundary area between the horizontal and inclined sliding surfaces can be expressed by (10):

$$\begin{aligned} N &= mv_1^2/r \\ N_h &= N \sin \varphi, f_h = \mu N \cos \varphi \\ \varphi &= x\theta/s \end{aligned} \quad (10)$$

where  $v_1$  is the incident velocity. Assuming that the resistant force maintains the same value during this process, the horizontal energy loss can be calculated by (11):

$$\begin{aligned} \Delta E(1) &= \int_0^s (N_h + f_h) dx \\ &= N \frac{1}{\theta/s} [(1 - \cos \theta) + \mu \sin \theta] \end{aligned} \quad (11)$$

By the energy conservation principle, the terminating horizontal velocity  $v_2$  when the particle reaches the end of the arc section can be determined by (12):

$$\begin{aligned} \Delta E(1) &= \frac{1}{2} mv_1^2 - \frac{1}{2} mv_2^2, \\ v_2 &= \sqrt{v_1^2 - 2\Delta E(1)} \end{aligned} \quad (12)$$

The average resistant force and the average velocity during this process can be taken as constants depending on the incident and terminating velocities. The corresponding friction force can also be determined and the energy dissipation can be calculated by computed friction force. Keeping this iterative operation until the error  $e$  is smaller than a tolerance of 0.01. The energy loss rate  $Q$  in the horizontal direction can be determined by (13).

$$\begin{aligned} \bar{N} &= m(v_1^2 + v_2^2)/2r \\ \Delta E(n) &= \bar{N} \frac{1}{\theta/s} [(1 - \cos \theta) + \mu \sin \theta] \\ e &= \frac{|\Delta E(n) - \Delta E(n-1)|}{\Delta E(n)} < 0.01 \\ Q &= \Delta E(n) / \frac{1}{2} mv_1^2 \end{aligned} \quad (13)$$

An example of this computation is given by the left plot in Fig. 3.3. For the parameters chosen in the present study, the energy loss rate is also shown by the right plot in Fig. 3.3. It

can be found that the energy loss rate during the area between horizontal and inclined sliding surfaces will increase with a larger inclined angle or a smaller radius. The range of the energy loss rate is found to be between 0.06 and 0.42 when the radius is reduced from 50mm to 10mm for a width of superimposed region of 10mm and a friction coefficient of 0.15.

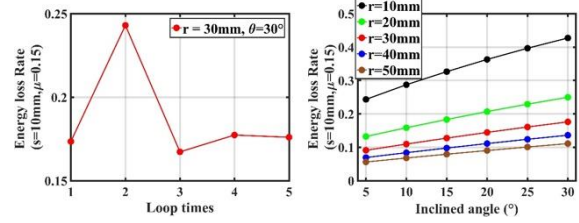


Fig. 3.3. The energy loss rate of simplified model from horizontal to inclined plane

If the change of vertical load component during the movement of the superstructure particle across the boundary area between inclined sliding surfaces is ignored, the resistant force will not contribute to the absorption of the horizontal energy. Therefore, the energy dissipation can be rewritten into (14), and the iterative procedure is the same as previously mentioned.

$$\begin{aligned} f &= \mu N \\ \Delta E(1) &= \int_0^s f dx = \mu N s \end{aligned} \quad (14)$$

An example result of above computation is given in the left plot in Fig. 3.4. The energy loss rate is also shown in the right plot in Fig. 3.4. It can be found that the energy loss rate during the boundary area between the inclined sliding surfaces will increase as the arc radius decreases. Due to the underlying assumption of the present model, the inclined angle between the sliding surfaces will not change the energy loss rate, which is controlled only by the width of the superimposed area. And the range of the energy loss rate is found to be between 0.045 and 0.2. It is observed that the horizontal energy dissipation rate is lower in the boundary area of the inclined sliding surfaces than that between the horizontal plane and the inclined sliding surface.

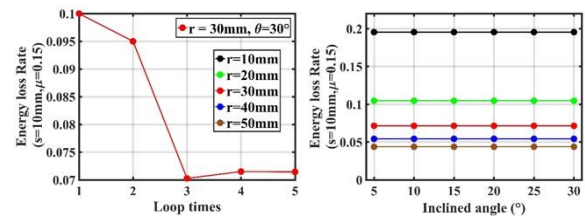


Fig. 3.4. The energy loss rate of simplified model between inclined sliding surfaces

The influence of the impact force effect on the superstructure particle displacement obtained by the nonlinear time-history analysis using 18 ground motion records is shown in Fig. 3.5. The plot indicates that the maximum displacements with different arc radii exhibit mostly 30% fluctuation compared with the maximum displacement without the impact effect, shown by the horizontal axis ( $r = \infty$ ). A more detailed plot is shown in Fig. 3.6, in which the average of the ratio between the results with and without the boundary area defined by (15) are plotted for various inclined angles.

$$R_r = \frac{1}{N_w} \sum_{i=1}^{N_w} \frac{D_{r,i}}{D_{No,i}} \quad (15)$$

where  $N_w$  is the number of records,  $D_{r,i}$  is the result of  $i$ -th record with the radius  $r$ ,  $D_{No,i}$  is the result of  $i$ -th record with the radius of infinity.

It is clearly shown that the average force ratio increases up to 8, as the inclined angle increases and the arc radius decreases. On the other hand, the average displacement response ratio tends to become smaller as the impact effect become greater, except for the case of radius of 10mm and an inclined angle of 30°. This is considered as the result of global influence of pounding when the impact effect becomes extremely severe.

○  $r = 10\text{mm}$  ●  $r = 20\text{mm}$  ○  $r = 30\text{mm}$  ●  $r = 40\text{mm}$  ○  $r = 50\text{mm}$  ---  $\pm 30\%$

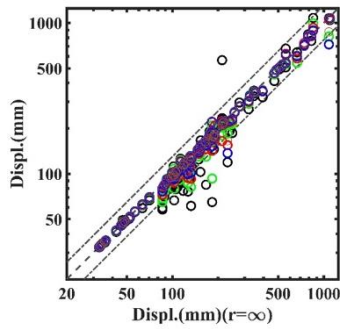


Fig. 3.5. The dispersion of displacement response under different radius

●  $r = 10\text{mm}$  ●  $r = 20\text{mm}$  ●  $r = 30\text{mm}$  ●  $r = 40\text{mm}$  ●  $r = 50\text{mm}$  ●  $r = \infty$

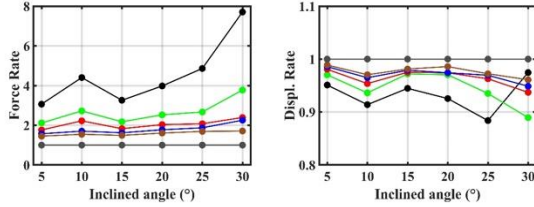


Fig. 3.6. The rate of max response under different radius

#### IV. QUANTITATIVE ANALYSIS

In the second step, a multiple spring model is used to describe the three-dimensional behavior of UPSS bearing and to confirm the results of the first step. Although the simplified model can describe the horizontal behavior of the Bidirectional UPSS with less uncertainties, the angle of the inclined sliding surfaces is the main feature to effectively provide restoring force in the event of strong ground motion, in which the vertical effect will be negligible. In such a situation, the multiple spring model allows a more reasonable description of the dynamic behavior in a quantitative manner.

The cross-section of the bidirectional UPSS has been already shown in Fig. 2.2. The cross-sections in longitudinal and transverse directions can be separated into three displacement regions, and are modelled by the corresponding spring elements as shown in Fig. 4.1. Each sliding surface consists of a combination of the normal and the sliding friction spring elements. In the study of unidirectional conditions of UPSS, additional impacting elements are introduced into the boundary areas between the horizontal and inclined surface to obtain a good agreement with the experimental results [2]. In

the Bidirectional UPSS, the influence of the assumed boundary condition between the inclined sliding surfaces is examined by introducing the same impacting elements into these areas. The longitudinal and transverse responses of the superstructure are then integrated including the circular coupled effect of friction force.

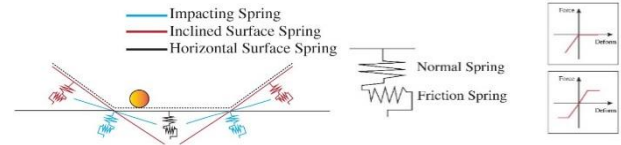


Fig. 4.1. Multiple spring model for sliding surfaces of UPSS

The Bidirectional UPSS model without introducing the impacting spring elements between the inclined surfaces is called the Bi-UPSS-regular model, while the model including the impacting spring elements between the inclined surfaces is referred to as the Bi-UPSS-added model in this study. Furthermore, the impacting spring elements in each cross-section and boundary areas expressed as overlapped sliding surfaces with  $\phi/2$  inclined angle, are treated in a similar manner to account for the corresponding coupled effect. The damping ratio for each sliding surface is set as 10%, except for the impacting spring elements as zero. The stiffness of the horizontal and inclined sliding surface elements are  $1.13 \times 10^7$  kN/m. The stiffness of the impacting spring elements is  $4.52 \times 10^7$  kN/m. The apparent friction coefficient of the impacting spring elements is 2.25 times as much as that of the sliding surfaces.

The ratios of the maximum response of Bi-UPSS-added model to that of Bi-UPSS-regular model obtained by the time-history analysis are shown in Fig. 4.2. The horizontal axis of the plot represents the inclined angle. The left plot indicates that the force response shows severer dispersion ranging from 0.6 to 1.6 than the displacement response shown in the right plot ranging in ratios between 0.8 and 1.2. On the other hand, although the mean value of the force ratios is higher in Bi-UPSS-added model, the mean value of displacement ratio is smaller in Bi-UPSS-added model. This observation of increased force and decreased displacement response with the consideration of the impact force effect coincides with the findings in the first step.

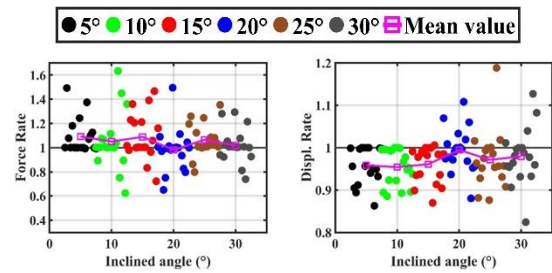


Fig. 4.2. The rate of Bi-UPSS-added to Bi-UPSS-regular models

The average ratios of the maximum response obtained by the analysis of the simplified model to that of Bi-UPSS-regular model are shown in Fig. 4.3. If the radius of the superimposed tubular arc is larger than 20mm, the maximum force response is mostly lower than the Bi-UPSS-regular model with the lowest rate being 0.5, except for the case of an arc radius of 10mm. On the other hand, the average displacement response is higher for the simplified model, implying that the simplified model may underestimate the

seismic performance of UPSS bearing. The reason may be the fact that the simplified model does not account for the actual vertical motion, the vertical energy dissipation and the detailed mechanical behavior which may provide extra displacement mitigation effects.

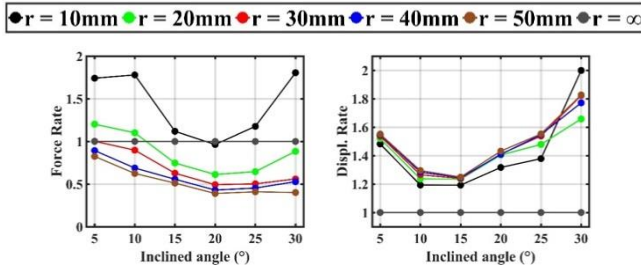


Fig. 4.3. The rate of maximum response of simplified model to Bi-UPSS regular model

#### V. POTENTIAL INFLUENCE OF IMPACT EFFECT IN BRIDGE SYSTEMS

In addition to the interest in the displacement response of the bearing, when the bidirectional UPSS is considered as a seismic performance enhancement approach used in the bridge systems, the protection performance for piers is even of greater importance. In this section, a span of a continuous girder bridge system with the implementation of bidirectional UPSS is used for the investigation of the effect of device application on the enhancement of seismic performance. The bridge system is comprised of the single pier, the girder and the bearing as shown in Fig. 5.1, in which an idealized two-lumped mass system is used to represent the system with two translational DOFs in the horizontal plane for the pier and two translational DOFs for the girder. The mass of the girder is 900t and that of the pier is 300t. The mechanical behavior of the RC pier is represented by the Clough degrading stiffness model independently in the longitudinal and transverse direction, with the yield strength corresponding to 0.66g lateral force. The initial stiffness of the RC pier is specified so that the elastic natural period for the non-isolated conditions becomes 0.5sec in both longitudinal and transverse directions. The degrading stiffness ratio is set as 0.05.

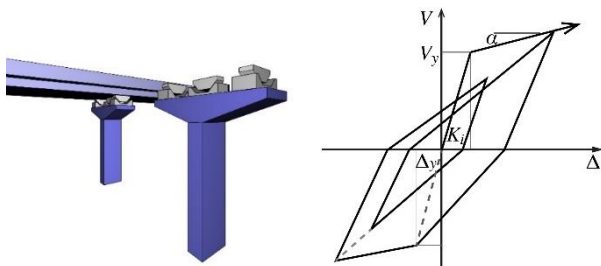


Fig. 5.1. Examined bridge system and Clough model of pier

The same set of parameters of Bidirectional UPSS model are used as in the previous sections. The relative bearing displacement and the response ductility factors of the pier are two concerned indices. Since the simplified model is proposed to examine the potential influence of impact effect, the numerical results may be totally unreliable in some extreme situation where the dynamic response is extremely sensitive to the incremental impact effect. It is considered to exclude these obviously unrealistic conditions. The obtained response expressed with the two indices are shown in the Fig. 5.2, compared with the case without the impact force effect. The maximum system responses are mostly located within the

range of 30%. This observation indicates that the introduction of impact effect may not significantly change the overall dynamic behavior of the system, excluding some exceptional cases. The average value of response ratios of the model with impact to that without impact is shown in Fig. 5.3. Decrease of the average bearing displacement of approximately 5% to 20% can be seen in the figure, while the average fluctuation in the response ductility factors of the pier is within the range of  $\pm 6\%$ . The influence of the impact effect on pier ductility turns out to be relatively minor.

○ r = 10mm ○ r = 20mm ○ r = 30mm ○ r = 40mm ○ r = 50mm ---  $\pm 30\%$

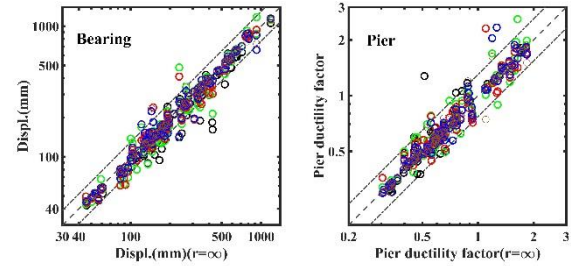


Fig. 5.2. The dispersion of displacement response under different radius

● r = 10mm ● r = 20mm ● r = 30mm ● r = 40mm ● r = 50mm ● r = ∞

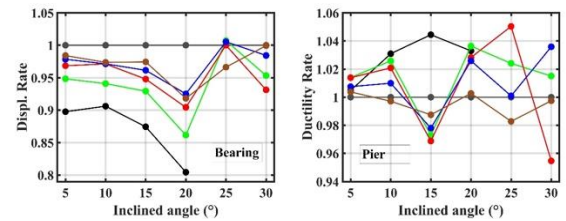


Fig. 5.3. The rate of max response under different radius

This conclusion can be further summarized in the Fig. 5.4 showing the relationship between the pier ductility factors and bearing displacements. There exists uncertainty, which is induced by the potential impact effect, on the evaluation of seismic performance especially in the pier response ductility factor.

● r = 10mm ● r = 20mm ● r = 30mm ● r = 40mm ● r = 50mm ● r = ∞

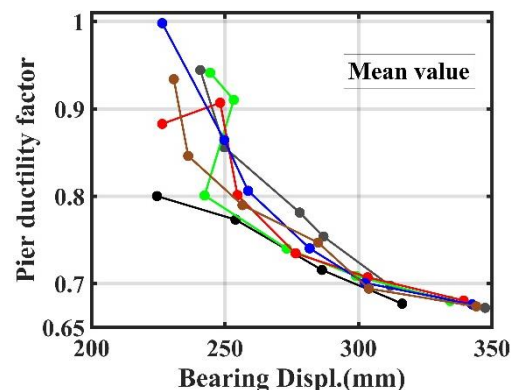


Fig. 5.4. The evaluation of seismic performance under different potential influence of impact effect

#### VI. CONCLUSIONS

The uncertainty introduced by the impact effect may cause difficulty in the practical application of UPSS bearings in the bidirectional condition. Since the impact effect in the

application of UPSS bearings is introduced by the boundary areas between the sliding surfaces, the potential influence of the impact effect of the Bidirectional UPSS on the bearing displacement and the pier response factor is investigated by seismic response analysis of the bidirectional UPSS models and bridge system model with different boundary conditions. In the first step, a simplified model is proposed to estimate the range of the structural parameters and the effect of the impact force in a controllable manner by introducing a tubular arc section with specific radii and the superimposed width into the boundary areas between the sliding surfaces for qualitative evaluation. In the second step, the multiple spring model of Bidirectional UPSS is used for quantitative evaluation of the impact force effect to provide a further practical description. Furthermore, the potential influence of impact effect on the pier response when bidirectional UPSS is implemented to a bridge system is investigated. The main findings obtained by this study can be summarized as follows:

- The potential impact effect in the bidirectional application of UPSS devices is modelled in a simplified model by the superimposed tubular arc section with a radius. The horizontal energy dissipation capacity of the impact effect can be explained by this model. The inclined angle between the sliding surface does not significantly change the energy loss rate, which is found to be between 0.045 and 0.2. It is observed that the horizontal energy dissipation rate is always larger in the horizontal-inclined boundary areas than the inclined-inclined boundary areas.
- The maximum displacement with different arc radii exhibit mostly 30% fluctuation compared with the maximum displacement without the impact effect.
- The tendency of the change of the displacement response due to the increasing intensity of impact effect in the simplified model is also shown by the analysis using the multiple spring model of bidirectional UPSS.
- It is found that the uncertainty of the average displacement of bidirectional UPSS is within 10% in the simplified model, and within 5% in the multiple spring model.
- The simplified model is likely to overestimate the displacement response comparing with the multiple spring model.
- In a simple bridge system with bidirectional UPSS application, the results of time-history analysis shows that, the introduction of impact effect may not significantly change the average behavior of the system, while the uncertainty in the evaluation of the seismic performance in terms of bearings displacement and pier response ductility are observed.

#### ACKNOWLEDGMENT

The study presented in this paper is conducted under the collaboration with the UPSS device development research group, and the result and investigation is accomplished based on the collective knowledge and discussion of the members of the research group. Contribution of Dr. Hiroshige Uno, Dr. Yukio Adachi (Hanshin Expressway Co. Ltd.), Dr. Tomoaki Sato (Hanshin Expressway Engineering Co. Ltd.), Prof. Taiji

Mazda (Kyushu Univ.), and members of JIP Techno Science Corp. is gratefully acknowledged.

#### REFERENCES

- [1] H. Otsuka, S. Unjoh, T. Terayama, J. Hoshikuma and K. Kosa, 'Damage to highway bridges by the 1995 Hyogoken Nanbu earthquake and the retrofit of highway bridges in Japan', *3rd U.S.-Japan workshop on Seismic Retrofit of Bridges*, Osaka, Japan, 10-11 December 1996.
- [2] Igarashi A, Shiraishi H. Seismic Response Control of Bridges Using UPSS Combined with Energy Dissipation Devices. *15th World Conference on Earthquake Engineering*, Lisbon, Portugal, 24-28 September (2012): Paper No.2280.
- [3] Sato, Tomoaki, et al. "Evaluation of Seismic Performance of Upss in Terms of Energy Dissipation Considering Nonlinear Pier Response." *Journal of Japan Society of Civil Engineers, Ser. A1 (Structural Engineering & Earthquake Engineering (SE/EE))* 69.4 (2013): 1\_609-1\_621 (in Japanese).
- [4] Igarashi, Akira, et al. "Investigation of Dynamic Behavior of Uplifting Slide Shoes by Shake Table Tests." *Journal of Japan Society of Civil Engineers, Ser. A1 (Structural Engineering & Earthquake Engineering (SE/EE))* 65.1 (2009): 426-433 (in Japanese).
- [5] Wolf, J. P., and P. E. Skrikerud. "Mutual pounding of adjacent structures during earthquakes." *Nuclear Engineering and Design* 57.2 (1980): 253-275.
- [6] Anagnostopoulos, Stavros A. "Pounding of buildings in series during earthquakes." *Earthquake engineering & structural dynamics* 16.3 (1988): 443-456.
- [7] Anagnostopoulos, Stavros A., and Konstantinos V. Spiliopoulos. "An investigation of earthquake induced pounding between adjacent buildings." *Earthquake engineering & structural dynamics* 21.4 (1992): 289-302.
- [8] Jankowski, Robert, Krzysztof Wilde, and Yozo Fujino. "Pounding of superstructure segments in isolated elevated bridge during earthquakes." *Earthquake engineering & structural dynamics* 27.5 (1998): 487-502.
- [9] Pant, Deepak R., and Anil C. Wijeyewickrema. "Performance of base-isolated reinforced concrete buildings under bidirectional seismic excitation considering pounding with retaining walls including friction effects." *Earthquake Engineering & Structural Dynamics* 43.10 (2014): 1521-1541.
- [10] Mavronicola, Eftychia A., Panayiotis C. Polycarpou, and Petros Komodromos. "Spatial seismic modeling of base-isolated buildings pounding against moat walls: effects of ground motion directionality and mass eccentricity." *Earthquake Engineering & Structural Dynamics* 46.7 (2017): 1161-1179.
- [11] Yu B, Becker T C, Sone T, et al. Experimental study of the effect of restraining rim design on the extreme behavior of pendulum sliding bearings[J]. *Earthquake Engineering & Structural Dynamics*, 2017, 47(4).
- [12] Hao H, Kaiming B I, Chou N, et al. STATE-OF-THE-ART REVIEW ON SEISMIC INDUCED POUNDING RESPONSE OF BRIDGE STRUCTURES[J]. *Journal of Earthquake & Tsunami*, 2013, 07(03):1350019-.
- [13] Banerjee A, Chanda A, Das R. Historical Origin and Recent Development on Normal Directional Impact Models for Rigid Body Contact Simulation: A Critical Review[J]. *Archives of Computational Methods in Engineering*, 2017, 24(2):397-422.
- [14] Goldsmith W, Frasier J T. Impact: The Theory and Physical Behavior of Colliding Solids[J]. *Journal of Applied Mechanics*, 1961, 28(4):639.
- [15] Maison B F, Kasai K. Analysis for a Type of Structural Pounding[J]. *Journal of Structural Engineering*, 1990, 116(4):957-977.
- [16] Maison, Bruce F., and Kazuhiko Kasai. "Dynamics of pounding when two buildings collide." *Earthquake engineering & structural dynamics* 21.9 (1992): 771-786.
- [17] Jing H S, Young M. Impact interactions between two vibration systems under random excitation[J]. *Earthquake Engineering & Structural Dynamics*, 1991, 20(7):667-681.
- [18] Davis R O. Pounding of buildings modelled by an impact oscillator[J]. *Earthquake Engineering & Structural Dynamics*, 1992, 21(3):253-274.
- [19] Pantelides C P, Ma X. Linear and nonlinear pounding of structural systems[J]. *Computers & Structures*, 1998, 66(1):79-92.

- [20] Chau K T, Wei X. X. Pounding of structures modelled as non-linear impacts of two oscillators[J]. *Earthquake Engineering & Structural Dynamics*, 2001, 30(5):633-651.
- [21] Muthukumar, Susendar, and Reginald DesRoches. "A Hertz contact model with non-linear damping for pounding simulation." *Earthquake engineering & structural dynamics* 35.7 (2006): 811-828.
- [22] Muthukumar, Susender, and Reginald Desroches. "Evaluation of impact models for seismic pounding." *Proceedings of the 13th World Conference on Earthquake Engineering, Vancouver, Canada*. 2004.
- [23] Chanda, Avishek, Arnab Banerjee, and Raj Das. "The application of the most suitable impact model (s) for simulating the seismic response of a straight bridge under impact due to pounding." *Int. J. Sci. Eng. Res* 7.2 (2016): 25-36.
- [24] Goyal S, Pinson E N, Sinden F W. Simulation of dynamics of interacting rigid bodies including friction I: General problem and contact model[J]. *Engineering with Computers*, 1994, 10(3):162-174.
- [25] Papadrakakis M, Apostolopoulou C, Zacharopoulos A, et al. Three-Dimensional Simulation of Structural Pounding during Earthquakes[J]. *Journal of Engineering Mechanics*, 1996, 122(5):423-431.
- [26] Klarbring A, Gunnar Bj, rkman. A mathematical programming approach to contact problems with friction and varying contact surface[J]. *Computers & Structures*, 1988, 30(5):1185-1198.
- [27] Dumont Y, Goeleven D, Rochdi M, et al. Frictional contact of a nonlinear spring[J]. *Mathematical & Computer Modelling*, 2000, 31(2):83-97.
- [28] Zhu P, Abe M, Fujino Y. Modelling three-dimensional non-linear seismic performance of elevated bridges with emphasis on pounding of girders[J]. *Earthquake Engineering & Structural Dynamics*, 2002, 31(11):1891-1913.
- [29] Glocker C. Concepts for modeling impacts without friction[J]. *Acta Mechanica*, 2004, 168(1-2):1-19.
- [30] Polycarpou P C, Papaloizou L, Komodromos P. An efficient methodology for simulating earthquake-induced 3D pounding of buildings[J]. *Earthquake Engineering & Structural Dynamics*, 2014, 43(7):985-1003.